**Luminescent Rare Earth based nanoparticles: a summarized overview of their synthesis, functionalization, and applications.**

Alberto Escudero,[1,2] Carolina Carrillo-Carrión,[3] Mikhail V. Zyuzin,[1] and Wolfgang J. Parak.[1,3]

1. AG Biophotonik, Fachbereich Physik, Philipps-Universität Marburg. Renthof 7. D-35037, Marburg, Germany.
2. Instituto de Ciencia de Materiales de Sevilla. CSIC – Universidad de Sevilla. C. Américo Vespucio 49. E-41092, Seville, Spain.
3. CIC biomaGUNE. Paseo Miramón 182. E-20009, San Sebastian, Spain.
* Corresponding author:

## Table of contents

**Abstract**

Rare earth-based nanoparticles are currently attracting wide research interest in Material Science, Physics, Chemistry, Medicine and Biology due to their optical properties, their stability and novel applications. We present in this review a summarized overview of the general and recent developments in their synthesis and functionalization. Their luminescent properties are also discussed, including the last advances in the enhancement of their emission luminescence. Some of their more relevant and novel biomedical, analytical, and optoelectronic applications are also commented.

## 1. Introduction, chemical composition, luminescent properties.

Rare earth (RE)-based nanoparticles (NPs) constitute one type of luminescent materials available in the literature. RE-based nanophosphors exhibit important advantages compared with the other available luminescent materials due to their lower toxicity, photostability, high thermal and chemical stability, high luminescence quantum yield, and sharp emission bands [1]. These nanophosphors usually consist of a host inorganic matrix doped with luminescent lanthanide (Ln) cations. The final characteristic and properties of the nanophosphors are highly influenced by both the inorganic matrix and the dopant. Fluoride matrices are used due to their low vibrational energies, which minimize the quenching of the exited state of the Ln cations and result in a higher quantum efficiency of luminescence [2-4]. Phosphate-based matrices attract interest for their high biocompatibility and good biodegradability [5]. Other matrices such as vanadates, molybdates, and wolframates are used to enhance the global luminescent emission of the materials [6-7], and some silicate-based matrices are appropriate for the production of persistent luminescent nanoparticles [8-9]. The election of the Ln cation or cations determines the final luminescent properties of the material. Luminescence is expected for most of the $Ln^{3+}$ cations, but in practice most of the studies are focused on $Eu^{3+}$, $Tb^{3+}$/$Ce^{3+}$, $Dy^{3+}$, and $Nd^{3+}$ cations, which produce red, green, yellow/orange luminescence, and near infrared luminescence, respectively [10-13]. These cations are examples of the so-called downconversion (DC) luminescence (i.e. conventional Stokes type), in which higher energy photons are converted into lower energy photons. High research attention is attracted by upconverting nanoparticles (UCNPs), in which the sequential absorption of two or more photons leads to the emission of light at shorter wavelength than the excitation wavelength (i.e. anti-Stokes type emission), which means that near infrared long-wavelength excitation radiation is converted into shorter visible wavelengths [14]. $Er^{3+}$, $Tm^{3+}$, and $Ho^{3+}$ codoped with $Yb^{3+}$ -, which acts as sensitizer, are commonly used as upconverting luminescent cations pairs [15]. The main disadvantage of Ln-doped NPs is their relatively low global intensity luminescence, caused by the low absorptions of the parity forbidden $Ln^{3+}$ 4f–4f transitions, and constituting a serious limitation for their use for different

applications [16]. Different energy transfers schemes from the host materials to the Ln cations are employed to enhance the global luminescence of downconverting lanthanide-doped NPs, which include the use of vanadate or oxyfluoride matrices [17-21]. Despite its highly scientific interest, even lower upconversion efficiencies are normally observed for UCNPs [22-23]. Core/shell nanostructures, which minimize the surface quenching effects [24-27], as well as the association with organic near infrared (NIR) dyes, which can alleviate the inherently weak and narrow near-infrared absorption of the Ln ions [28], are used to enhance the luminescence of such materials. However, laser excitation sources are still required to study these particles.

In this article the more recent and common synthetic methods of luminescent NPs based on RE will be briefly summarized, as well as the different existing functionalization strategies. Some of their imaging, sensing, and optoelectronic applications will also be mentioned. For a deeper and more detailed description some excellent reviews can be found in the recent literature [15, 29-33].

## 2. Synthesis of uniform luminescent nanoparticles

Thermal decomposition [34], coprecipitation [2, 35], cation exchange [36], and hydro(solvo)thermal synthesis have become popular routes for the preparation of monodisperse Ln-doped luminescent NPs. Among the latters, a general synthesis strategy based on a phase transfer and separation mechanism occurring at the interfaces of the liquid, solid and solution (LSS) phases during the synthesis normally produces small Ln-doped inorganic nanoparticles with a narrow particle size distribution, a high luminescence efficiency, and a high phase purity of the particles [37]. These syntheses are carried out in organic solvents (such as oleic or linoleic acids, ethanol, octadecene, eicosene, trioctylamine) in presence of additives such as sodium oleate, sodium linoleate, trioctylphosphine oxide (TOPO), and stearic acid at high temperatures (200 – 400 ºC) [38-40]. However, the hydrophobic nature of the resulting NPs requires a further step of surface modification to make them water-dispersible. Water dispersible NPs with controlled size and shape can be synthesised by recently reported methods based

on homogeneous precipitation in polyol-based solvents at moderate temperatures (120-180 ºC). These strategies include an optimization of the different reaction parameters, such as solvents (including mixtures of them), precursors, concentrations, temperature and presence of additives. Many different luminescent and uniform Ln-doped inorganic NPs, including fluorides [41-44], phosphates [45-48], and vanadates [19, 21] have been reported. Microwave-assisted methods in both water and polyol-based solvents have also been described, resulting in much shorter reaction times [49-50]. Some examples of monodisperse Ln-doped NPs are shown in Figure 1.

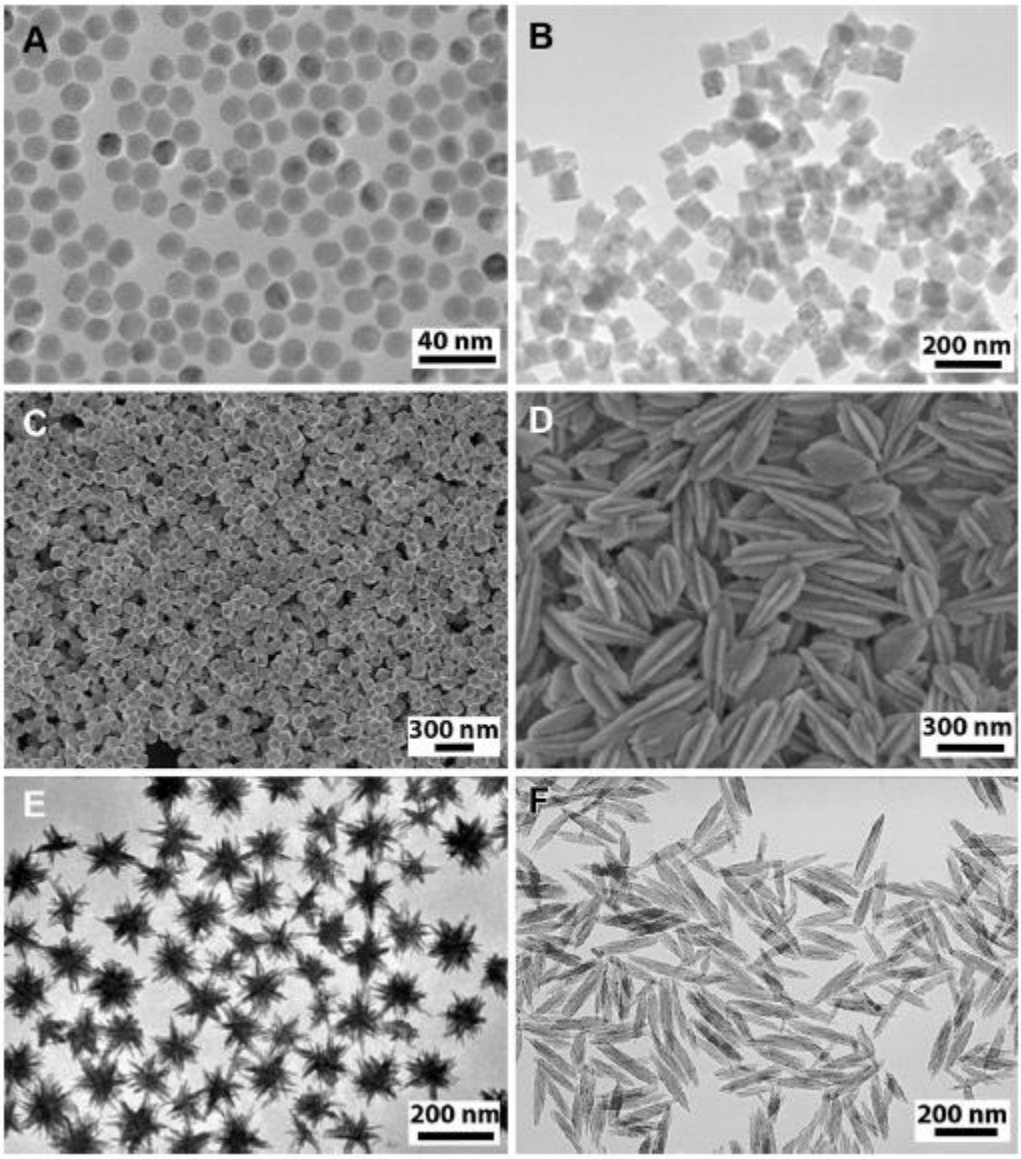


Figure 1 A: $Ho^{3+}$, $Yb^{3+}$-doped $NaGdF_4$ NPs synthesised in oleic acid and 1-octadecene at 340 ºC. Taken from [40]. B: $Eu^{3+}$-doped $GdPO_4$ nanocubes synthesised in butylene glycol at 120 ºC, taken from [45]. C: $Eu^{3+}$-doped $\alpha$-$BiO_yF_{3-2y}$ NPs with octahedrical morphology synthesised in diethyleneglycol-water at 120 ºC. Taken from [18]. D: $Dy^{3+}$-doped $GdPO_4$ particles with a lance-

shaped morphology synthesised in ethylene glycol-water at 180 ºC. Taken from [46]. F: $Eu^{3+}$-doped $BiPO_4$ nanostars synthesised in ethylene glycol-water in presence od sodium citrate at 120 ºC. Taken from [47]. F: $Eu^{3+}$-doped calcium hydroxyapatite nanospindles synthesised in water at 180 ºC in presence of PAA. Taken from [49].

Recently, laser ablation of micrometric sized powder Ln-doped particles has been used to produce Ln-doped NPs with a great control of their size and monodispersity [51].

## 3. Functionalization and colloidal stability

A functionalization process is especially required for the biomedical use of NPs, and it is mandatory for non water-dispersible nanoparticles. Functionalization not only increases the colloidal stability of the NPs by introducing electrostatic and/or steric repulsions [52], but also provides anchors for adding functional ligands of biomedical interest such as antibodies, peptides, proteins, and some anticancer drugs [53]. Ligand exchange, polymer encapsulation and silica encapsulation are common strategies used for the stabilization in water of native hydrophobic NPs. In the ligand exchange method, the original hydrophobic ligands are completely displaced by hydrophilic ligands (i.e. PEG-type and polymeric ligands, and anions such as citrate and $BF_4^-$) on the NP surface [54-55]. Ligand exchange methods typically offer NPs with smaller hydrodynamic diameters but suffer (for most NP materials) from limited colloidal stability. Polymer coating yields NPs that are very colloidally stable, but they normally show larger hydrodynamic radii [56]. In this strategy, the hydrophobically capped NPs are overcoated with amphiphilic polymers such as poly(isobutylene-alt-maleic anhydride) modified with dodecylamine (PMA), and its modifications with 4-(aminomethyl)pyridine (Py-PMA), and polyelthylene glycol (PEG-PMA) [54, 57-59]. The hydrophobic portion of the polymer intercalates with the hydrophobic ligands on the NP surface leaving the hydrophilic portion of the polymer exposed to solution [56]. Treatments with acids [60] or with excess of ethanol under ultrasonication [61] have also been used to remove the hydrophobic organic coating of the nanoparticles, and the -oleic acid ligands on the nanoparticles can be oxidized with the Lemieux-von Rudloff reagent, yielding water-dispersible carboxylic acid-functionalized NPs [62].

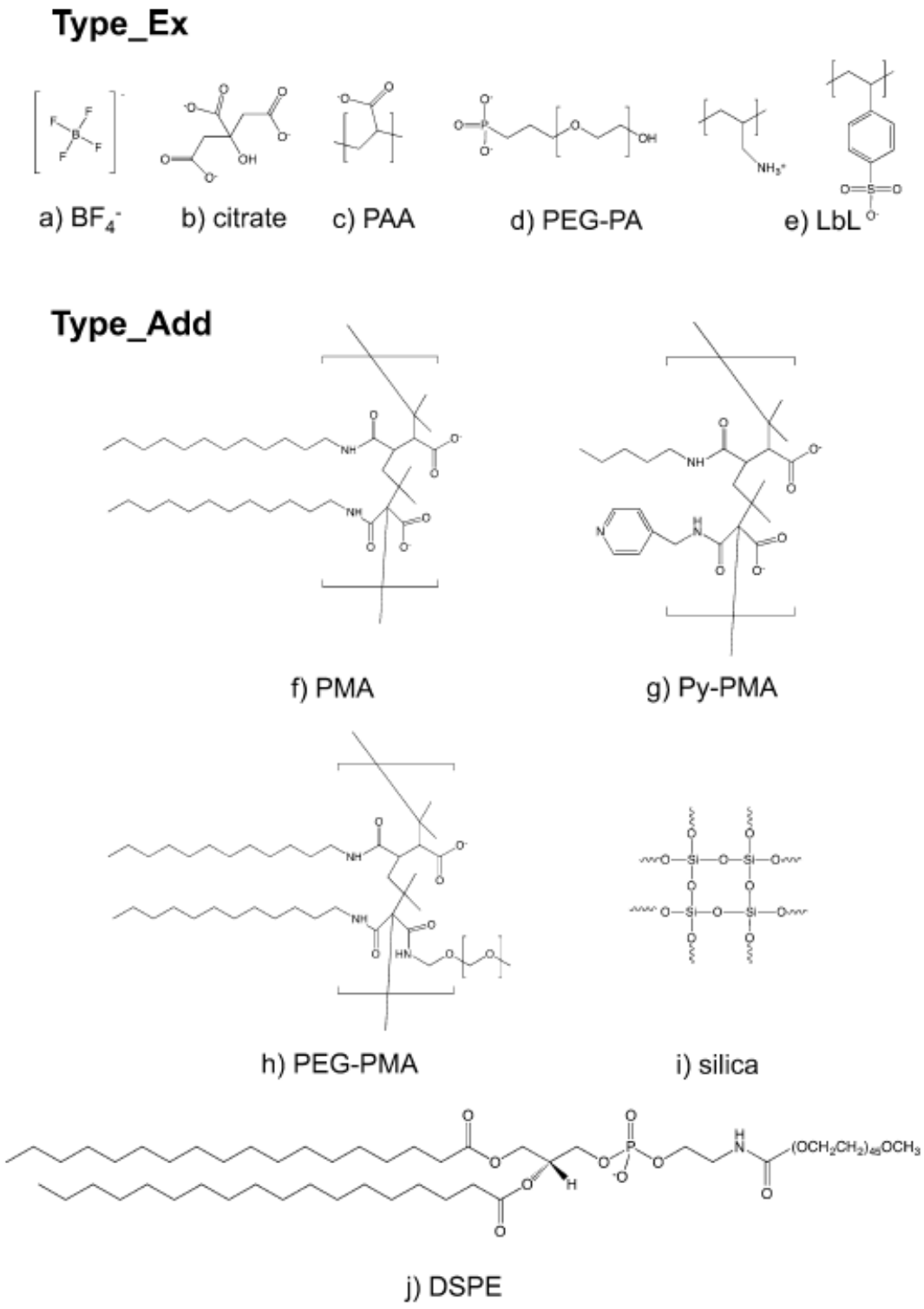


Figure 2: Overview of general strategies for surface modification of Ln-doped nanoparticles. The modifications can be classified into two categories: (a)–(e) ligand exchange methods (Type_Ex); (f)–(j) addition of an amphiphilic layer or silica coating (Type_Add). Examples of Type_Ex modifications include coating with: (a) tetrafluoroborate ($BF_4^-$); (b) trisodium citrate (citrate); (c) poly(acrylic acid) (PAA); (d) poly(ethylene-oxide)-10-OH with a terminal phosphate ester (PEG-PA); (e) layer-by-layer coating with poly(sodium 4-styrenesulfonate) (PSS) and poly(allylamine

hydrochloride) (PAH) (LbL) on an initial citrate layer. Examples of Type_Add modifications are coating with: (f) poly(isobutylene-*alt*-maleic anhydride) modified with dodecylamine (PMA); (g) the same as (f) but with a further modification with 4-(aminomethyl)pyridine (Py-PMA); (h) the same as (f) but with further modification with α-methoxy-ω-amino poly(ethylene glycol)-1200 (PEG-PMA); (i) silica coating with a shell thickness of ~5 nm (silica); (j) 1,2-distearoyl-*sn*-glycero-3-phospho-ethanolamine-*N*-[methoxy(poly-ethylene glycol)-2000] (ammonium salt) (DSPE). Taken from [54].

The more convenient strategy of functionalization of hydrophilic Ln-doped NPs is the so-called one-pot synthesis, in which the functionalising agent acts as additive during the synthesis process. In some cases, their presence plays also a key role in the final morphology of the particles [49]. One-pot synthesis of luminescent Ln-doped NPs with aminocaproic and citric acid [63], poly-ethylenimine (PEI)[64] and poly acrylic acid (PAA) [19, 21, 43] have been recently reported in the literature. Functionalization of Ln-doped NPs can also be carried out in a second step with agents such as and dextran-based polymers [19, 42]. The Layer-by-layer (LbL) approach, which is based on the electrostatic deposition of layers of polyelectrolytes with alternating charge on the surface of the particles [65], has also been used for the functionalization of RE fluoride [54, 66] and vanadate NPs [67]. However, NPs functionalised in a second step normally show a worse colloidal stability, when compared with the one-pot synthesised [67]. Silica-shell encapsulation (i.e. the growth of a silica shell around the NP) is used to functionalize both hydrophobic and hydrophilic NPs [68]. The reverse microemulsion method can be applied for hydrophobic nanoparticles [69], whereas the standard Stöber procedure is used for hydrophilic NPs, which in some cases have however to be previously stabilized with agents such as polyvinylpyrrolidone (PVP) of PEG-based ligands [70-71]. This functionalization process shows some advantages, given the $SiO_2$ high biocompatibility and possible further surface chemistry, which can be used to link different molecules of biomedical interest. A summary of some possible functionalization strategies is shown in Figure 2.

## 4. Bioimaging applications

Both downconverting and upconverting Ln-doped NPs can be used for bioimaging applications, although their use is highly limited by their low global luminescent emission. For the DC nanophosphors, the direct excitation of the $Ln^{3+}$ cations (which normally consists of narrow and low absorbance bands, the more intense occurring at 393 nm for $Eu^{3+}$, 349 and 366 for $Tb^{3+}$, and 349 for $Dy^{3+}$) is normally not enough to produce intense luminescence. As mentioned above, this can be overcome though an indirect excitation through the matrix, but still ultraviolet excitations radiations are required, which in somehow can be harmful for the cells.

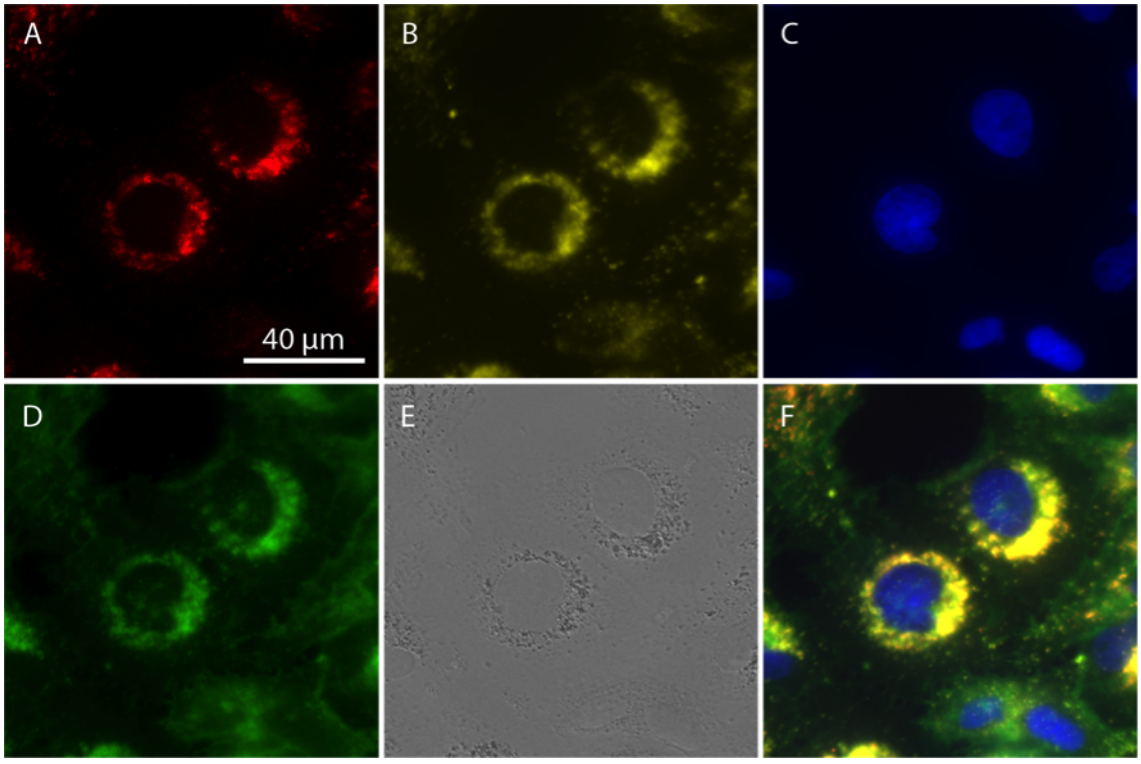


Figure 3: Fluorescence images of HeLa cells incubated with $Eu^{3+}$, $Bi^{3+}$ - doped $YVO_4$ NPs for 24 h. (A) Red channel, nanoparticles ($\lambda_{ex}$ = 340 ± 26 nm; $\lambda_{em}$ > 600 nm) (B) yellow channel, lysosomes; (C) blue channel, cell nuclei; (D) green channel, cell membranes; (E) transmission image, and (F) merged image. The luminescence of B to D is due cell inmunostaining with organelle-specific dyes. Taken from [67].

Recently, $Eu^{3+}$, $Bi^{3+}$ codoped $REVO_4$ (RE = Y, Gd) NPs have been proposed for *in vitro* bioimaging applications (Figure 3) [67]. The incorporation of $Bi^{3+}$ into the $REVO_4$ structure shifts the original absorption band corresponding to the vanadate

toward longer wavelengths, yielding nanophosphors excitable by near-ultraviolet and visible light. More studies can be found in the literature regarding UCNPs, since the use of near infrared light for excitation avoids photodamage, background fluorescence in biological systems and enables a higher penetration depth into biological tissue [33]. UCNPs do not show intermittent emission (blinking) upon continuous excitation, and they can be even used for long--term imaging due to their photostability [72]. These entire features make them highly attractive for bioimaging applications in both *in vitro* and *in vivo* [73-77] (Figure 4).

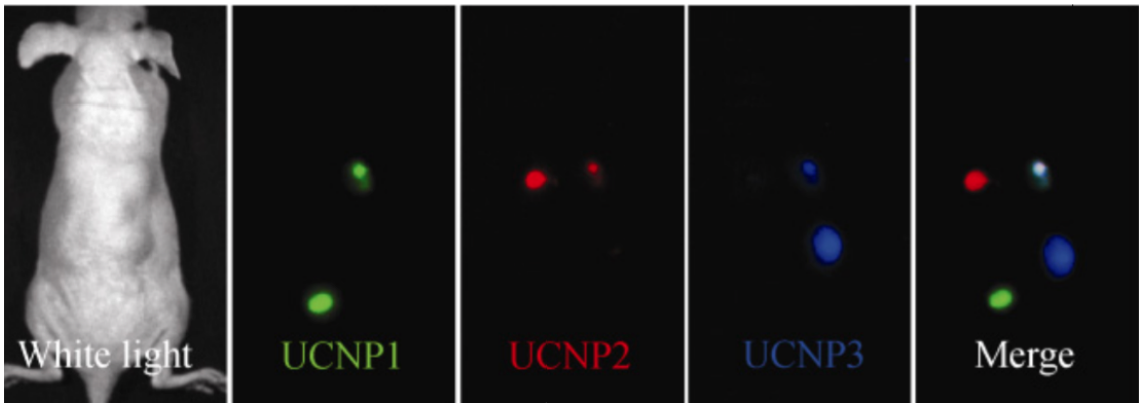


Figure 4: Left: A white light image of a mouse subcutaneously injected with different $Er^{3+}$, $Yb^{3+}$-doped $NaYF_4$ UCNPs; Rest of the images: *in vivo* multicolor images of a nude mouse subcutaneously injected with different UCNPs solutions. Taken from [74].

## 5. Sensing and analytical applications.

Application of Ln-doped NPs for sensing can be roughly divided into two classes: one is the directly observed luminescence from the Ln-doped NPs, and the other is based on fluorescence resonance energy transfer (FRET). An important feature of Ln-doped NPs for using their direct intrinsic fluorescence is that they present multiple emission lines, which allows ratiometric measurements because normally some of them are analytically sensitive, while others are insensitive and serve as reference signal [78]. Ln-doped NPs can also be coupled with organic fluorophores, metallic nanoparticles or quantum dots for FRET-based sensing approaches, where Ln-doped NPs are typically the donor unit. For providing selective detection towards a specific analyte (e.g. biomolecules, ions, gas molecules), the NPs have to be functionalized with suitable groups/motifs that have a recognition capability of

the target analyte. For example a single-stranded DNA has been used as $Hg^{2+}$-capturing element in the development of a method for determining $Hg^{2+}$ ions based on a FRET mechanism between $Tm^{3+}$, $Yb^{3+}$-doped $NaYF_4$ UCNPs as energy donor and a DNA intercalating dye (SYBR Green I) as energy acceptor [79]. As the SYBR has a strong absorbance overlapping with the blue emission of the UCNPs, in presence of $Hg^{2+}$ ions there is a simultaneous decrease of the blue emission of the UCNPs and an increase of SYBR green emission. By monitoring the ratio of the acceptor emission to the donor emission, the $Hg^{2+}$ ion can be detected at levels as low as 0.06 nM. This system allows not only determining the concentration of $Hg^{2+}$ but also monitoring changes in the distribution of $Hg^{2+}$ in living cells by upconversion luminescence bioimaging.

Using Au NPs as acceptor instead of a fluorophore, the detection of trace amounts of avidin has been reported. In this system the selective and sensitive avidin-biotin interaction is the responsible for bringing together the avidin-modified $Er^{3+}$, $Yb^{3+}$-doped $NaYF_4$ NPs used as donor and the biotinylated-Au NPs, whose strong absorption at ~541 nm matches well with the green emission of the Ln-doped NPs, and therefore an effective FRET process occurs [80]. An important advantage of this approach is its potential to be extended to wherever the avidin-biotin system, for example to study protein-proteins interactions, ligand-receptor interactions, the formation of DNA duplexes and so on.

Looking for a higher efficiency of the FRET process, and thus a higher sensitivity of the method, Liu *et al.* proposed the use of graphene oxide (GO) as efficient acceptor, since it quenches totally the visible emissions of the RE-NPs due to their ultrahighly strong absorption [81]. After quenching the emission from single-stranded DNA-functionalized $Er^{3+}$, $Yb^{3+}$-doped $NaYF_4$ NPs by their adsorption on the surface of GO their fluorescence can be recovered by addition of adenosine triphosphate (ATP) (Figure 5). ATP causes the desorption of the ssDNA-NPs from the GO as consequence of the formation complexes of ATP with the ssDNA (designed as adenosine triphosphate-specific aptamer), resulting in the decreased quenching efficiency and enhanced upconversion fluorescence which is

proportional to the ATP concentration. This aptasensor design can be further extended for sensing other kinds of molecules.

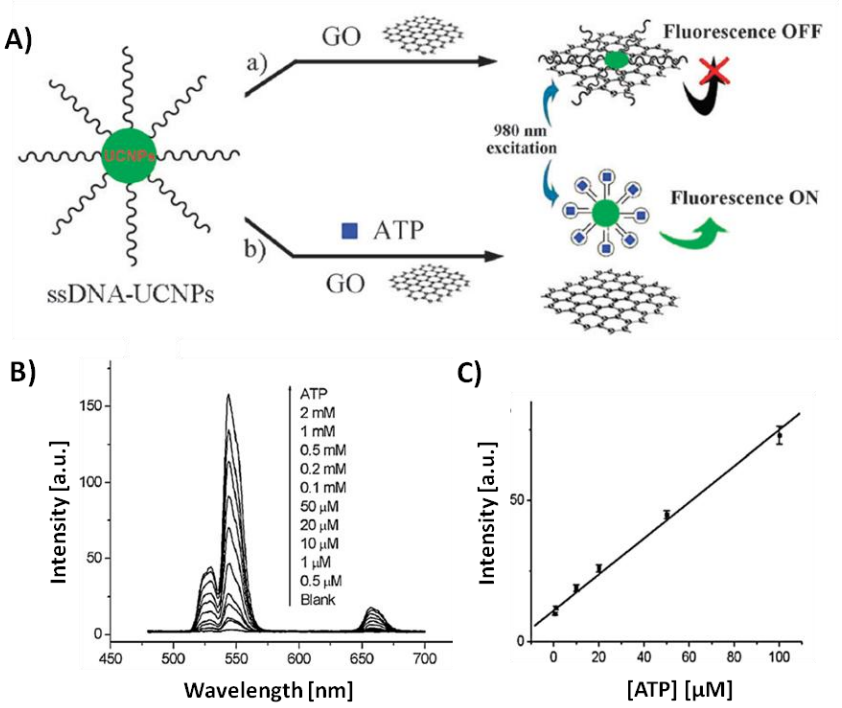


Figure 5: (A) Scheme of the upconversion fluorescence resonance energy transfer between ssDNA-UCNPs and GO for ATP sensing. (B) Upconversion fluorescence spectra of the UCNPs-GO FRET aptasensor in the presence of 0–2 mM ATP. (C) Plot of upconversion fluorescence intensity at 547 nm vs. ATP concentration. Taken from [81].

Semiconductor QDs have also been combined with UPCNPs in FRET configurations. The superiority of QDs as acceptors is owing to the fact that they have broad excitation bands and size-tunable emission wavelength, and thus the upconversion wavelength of UCNP–QD couple may be continuously adjusted. Combining $Tm^{3+}$, $Yb^{3+}$-doped $NaYF_4$ NPs as the energy donor and the CdTe QDs as the energy acceptor, the determination of lead ions in human serum with a detection limit of 80 nM has been achieved [82]. Such low detection limit is possible thanks to the use of NIR-laser as excitation source, which is capable of overcoming self-luminescence from serum excitation with visible light.

A FRET process is not only possible between two NPs, but also between the emission bands of RE NPs and an enzyme absorbance band. $Tm^{3+}$, $Yb^{3+}$-doped

$Gd_4O_2S$ NPs have been used to monitor the redox state of a flavoenzyme (PETNR, pentaerythritol tetranitrate reductase) [83]. Due to a variation in the absorbance profile of the flavin core of the enzyme upon reduction/oxidation, the FRET between the two can effectively be turned 'on' or 'off' by changing the redox state of PETNR. The presence of two bands separated by over 300 nm allowed the ratiometric signalling of this process.

The multiplexing capabilities of Ln-doped NPs have been also demonstrated by using different UCNPs excited with the same IR laser. The simultaneous detection of two types pathogenic bacteria (Salmonella Typhimurium and Staphylococcus aureus) was carried out by means of aptamer-conjugated $Er^{3+}$, $Yb^{3+}$, and $Tm^{3+}$, $Yb^{3+}$- doped $NaYF_4$ UCNPs [84].

Interestingly, Ln-doped UCNPs can also be used as nanothermometers based on the strong temperature dependence of the fluorescence intensities from two emitting levels of lanthanides [85-86]. This principle has been exploited for monitoring temperature changes in living cells, which is of particular interest for the investigation of enzyme reactions and sub-cellular processes [87]. Wolfbeis *et al.* studied temperature sensing using UCNPs of varying size and RE dopants recently [88]. They found that the core-shell structured hexagonal 2% $Er^{3+}$, 20% $Yb^{3+}$-doped $NaYF_4/NaYF_4$ UCNPs were more suitable for temperature sensing because their higher brightness allowed resolving temperature differences of less than 0.5 °C in the physiological range between 20 and 45 °C [88].

## 6. Optoelectronic applications

Because of their unique optical properties, lanthanide-doped materials are also widely used for optoelectronic applications, which include laser sources [89], fiber-optic communication [90], light-emitting diodes and solid-state lighthening [91-92], and color display devices [93]. These properties have been extensively studied in bulk materials since the last century, and nowadays the design and the study of the properties and applications of the nanostructured materials attracts

wide research interest. In particular Ln-doped semiconductor nanostructures open up possibilities for photonic/electronic integration and cheap CMOS-compatible optical sources, while efficient solid-state lighting based on Ln-doped nanostructures are increasingly playing a role in new green technologies [94].

Some Ln-doped NPs are used as color and white light-emitting materials. For the latter, both the selection of appropriate host matrices, which should be able to excite the Ln cations after one single wavelenght absorpion, and the optimization of the Ln contents, which can also absorb and transfer energy between them, are demanded. Examples of Ln-doped white light-emitting NPs are $Dy^{3+}$, $Eu^{3+}$ - doped $ZrO_2$ [95], $Dy^{3+}$-doped yttria stabilized zirconia (YSZ) [96], and $Dy^{3+}$, $Tb^{3+}$, $Eu^{3+}$ - doped $GdVO_4$ [46].

Ln-doped NPs are also used to improve the energy conversion efficiency in solar cells by both overcoming the two primary loss mechanisms in solar cells. Such mechanisms are related to the absorption of photons with larger or lower energy than the bandgap of the solar cell, reducing in practice their efficiecy. On one hand, DC NPs can absorb UV photons and re-emit them at longer wavelengths, where the solar cell exhibits a significantly better response [97]. For example, $Eu^{3+}$, $Bi^{3+}$-doped $YVO_4$ NPs have been used in Si-based solar cells to reduce the thermalization of charge carriers caused by the absorption of high-energy photons [98]. On the other hand, UCNPs are used to transform low energy photons into higher energy photons, that can be used by the solar cells, and thus significantly enhance the efficiency of the photovoltaic device [99]. $Er^{3+}$, $Yb^{3+}$-doped $NaYF_4$ NPs, one of the most studied fluorides, has been used with this objective [100]. In some cases, UCNPs are also associated with organic dyes [101].

## 7. Concluding remarks and future outlook

Current and widely used strategies for synthesis and functionalization of Ln-based NPs have been discussed, and some recent advances in their imaging, sensing, and optoelectronic applications have been mentioned. Even when the synthesis in organic media, normally in presence of additives such as oleic acid, provides a

powerful tool for the production of highly monodisperse NPs, the hydrophobic character of the resulting NPs requires the development of new synthesic routes for yielding homogeneous, uniform, and water-dispersible nanoparticles. The use of polyol-based solvents in homogeneous precipitation reactions at moderate temperatures has partially overcome this disadvantage, although NPs sizes are larger (>25 nm). New synthesis methods yielding Ln-doped NPs with different shapes and sizes for many systems are still demanded, as well as universal functionalization strategies for hydrophilic NPs, as the Layer-by-Layer approach. Apart from the synthesis and functionalization perspectives, the main disadvantage of Ln-based NPs continues being their relative low emission intensity. Even when the indirect excitation with codoped inorganic matrices for downconverting NPs and core/shell structures for upconverting NP have demonstrated notable improvements, new strategies to enhance their luminescence are still demanded.

**Acknowledgements**

This work was supported by a Junta de Andalucía (Spain) Talentia Postdoc Fellowship, co-financed by the European Union's Seventh Framework Programme, grant agreement no 267226, and by the European Commission (grant FutureNanoNeeds to WJP). CCC acknowledges the Spanish Ministry of Economy and Competitiveness for a Juan de la Cierva–Incorporacion contract.

## 8. References


1. Wang GF, Peng Q, Li YD (2011) Accounts of Chemical Research 44: 322
2. Stouwdam JW, van Veggel FCJM (2002) Nano Lett. 2: 733
3. Lage MM, Righi A, Matinaga FM, Gesland JY, Moreira RL (2004) Journal of Physics: Condensed Matter 16: 3207
4. Yan RX, Li YD (2005) Advanced Functional Materials 15: 763
5. Epple M, Ganesan K, Heumann R, Klesing J, Kovtun A, Neumann S, Sokolova V (2010) J. Mater. Chem. 20: 18
6. Gupta BK, Rathee V, Narayanan TN, Thanikaivelan P, Saha A, Govind, Singh SP, Shanker V, Marti AA, Ajayan PM (2011) Small 7: 1767
7. Kaczmarek AM, Van Deun R (2013) Chemical Society Reviews 42: 8835
8. Maldiney T, Richard C, Seguin J, Wattier N, Bessodes M, Scherman D (2011) ACS Nano 5: 854
9. Maldiney T, Lecointre A, Viana B, Bessière A, Bessodes M, Gourier D, Richard C, Scherman D (2011) J. Am. Chem. Soc. 133: 11810
10. Richardson FS (1982) Chem. Rev. 82: 541
11. Liping L, Minglei Z, Wenming T, Xiangfeng G, Guangshe L, Liusai Y (2010) Nanotechnology 21: 195601
12. Eliseeva SV, Bunzli J-CG (2010) Chemical Society Reviews 39: 189
13. Riedinger A, Zhang F, Dommershausen F, Rocker C, Brandholt S, Nienhaus GU, Koert U, Parak WJ (2010) Small 6: 2590
14. Wang F, Liu X (2009) Chemical Society Reviews 38: 976
15. Haase M, Schäfer H (2011) Angewandte Chemie International Edition 50: 5808
16. Wisser MD, Chea M, Lin Y, Wu DM, Mao WL, Salleo A, Dionne JA (2015) Nano Lett. 15: 1891
17. Núñez N, Sabek J, García-Sevillano J, Cantelar E, Escudero A, Ocaña M (2013) Eur. J. Inorg. Chem. 2013: 1301
18. Escudero A, Moretti E, Ocaña M (2014) CrystEngComm 16: 3274
19. Núñez NO, Rivera S, Alcántara D, de la Fuente JM, García-Sevillano J, Ocaña M (2013) Dalton Trans. 42: 10725
20. Abdesselem M, Schoeffel M, Maurin I, Ramodiharilafy R, Autret G, Clément O, Tharaux P-L, Boilot J-P, Gacoin T, Bouzigues C, Alexandrou A (2014) ACS Nano 8: 11126
21. Núñez NO, Zambrano P, García-Sevillano J, Cantelar E, Rivera-Fernández S, de la Fuente JM, Ocaña M (2015) Eur. J. Inorg. Chem. 2015: 4546
22. Boyer J-C, van Veggel FCJM (2010) Nanoscale 2: 1417
23. Mialon G, Türkcan S, Dantelle G, Collins DP, Hadjipanayi M, Taylor RA, Gacoin T, Alexandrou A, Boilot J-P (2010) The Journal of Physical Chemistry C 114: 22449
24. Shao W, Chen G, Damasco J, Wang X, Kachynski A, Ohulchanskyy TY, Yang C, Ågren H, Prasad PN (2014) Opt. Lett. 39: 1386
25. Yin W, Zhou L, Gu Z, Tian G, Jin S, Yan L, Liu X, Xing G, Ren W, Liu F, Pan Z, Zhao Y (2012) J. Mater. Chem. 22: 6974
26. Punjabi A, Wu X, Tokatli-Apollon A, El-Rifai M, Lee H, Zhang Y, Wang C, Liu Z, Chan EM, Duan C, Han G (2014) ACS Nano 8: 10621
27. Dantelle G, Calderón-Villajos R, Zaldo C, Cascales C, Gacoin T (2014) ACS Applied Materials & Interfaces 6: 22483

28. Zou W, Visser C, Maduro JA, Pshenichnikov MS, Hummelen JC (2012) Nat Photon 6: 560
29. Dong H, Du S-R, Zheng X-Y, Lyu G-M, Sun L-D, Li L-D, Zhang P-Z, Zhang C, Yan C-H (2015) Chem. Rev. 115: 10725
30. Liu Y, Tu D, Zhu H, Ma E, Chen X (2013) Nanoscale 5: 1369
31. Wang G, Peng Q, Li Y (2011) Accounts of Chemical Research 44: 322
32. Gnach A, Bednarkiewicz A (2012) Nano Today 7: 532
33. Sedlmeier A, Gorris HH (2015) Chemical Society Reviews 44: 1526
34. Boyer J-C, Vetrone F, Cuccia LA, Capobianco JA (2006) J. Am. Chem. Soc. 128: 7444
35. Yi GS, Chow GM (2006) Advanced Functional Materials 16: 2324
36. Dong C, van Veggel FCJM (2009) ACS Nano 3: 123
37. Wang X, Zhuang J, Peng Q, Li Y (2005) Nature 437: 121
38. Wang F, Deng R, Liu X (2014) Nat. Protocols 9: 1634
39. Zhengquan L, Yong Z (2008) Nanotechnology 19: 345606
40. Naccache R, Vetrone F, Mahalingam V, Cuccia LA, Capobianco JA (2009) Chem. Mat. 21: 717
41. Quintanilla M, Nunez NO, Cantelar E, Ocana M, Cusso F (2011) Nanoscale 3: 1046
42. Rodríguez-Liviano S, Núñez NO, Rivera-Fernández S, de la Fuente JM, Ocaña M (2013) Langmuir 29: 3411
43. Nuñez NO, García M, García-Sevillano J, Rivera-Fernández S, de la Fuente JM, Ocaña M (2014) Eur. J. Inorg. Chem. 2014: 6075
44. Becerro AI, González-Mancebo D, Cantelar E, Cussó F, Stepien G, de la Fuente JM, Ocaña M (2016) Langmuir 32: 411
45. Rodríguez-Liviano S, Becerro AI, Alcántara D, Grazú V, de la Fuente JM, Ocaña M (2013) Inorg. Chem. 52: 647
46. Becerro AI, Rodríguez-Liviano S, Fernández-Carrión AJ, Ocaña M (2013) Cryst. Growth Des. 13: 526
47. Becerro AI, Criado J, Gontard LC, Obregón S, Fernández A, Colón G, Ocaña M (2014) Cryst. Growth Des. 14: 3319
48. Becerro AI, Ocana M (2015) RSC Advances 5: 34517
49. Escudero A, Calvo ME, Rivera-Fernández S, de la Fuente JM, Ocaña M (2013) Langmuir 29: 1985
50. Rodríguez-Liviano S, Aparicio FJ, Rojas TC, Hungría AB, Chinchilla LE, Ocaña M (2012) Cryst. Growth Des. 12: 635
51. Gemini L, Hernández MC, Kling R (2016), vol 9722
52. Pellegrino T, Kudera S, Liedl T, Muñoz Javier A, Manna L, Parak WJ (2005) Small 1: 48
53. Thanh NTK, Green LAW (2010) Nano Today 5: 213
54. Wilhelm S, Kaiser M, Wurth C, Heiland J, Carrillo-Carrion C, Muhr V, Wolfbeis OS, Parak WJ, Resch-Genger U, Hirsch T (2015) Nanoscale 7: 1403
55. Dong A, Ye X, Chen J, Kang Y, Gordon T, Kikkawa JM, Murray CB (2011) J. Am. Chem. Soc. 133: 998
56. Zhang F, Lees E, Amin F, Rivera_Gil P, Yang F, Mulvaney P, Parak WJ (2011) Small 7: 3113
57. Li L-L, Zhang R, Yin L, Zheng K, Qin W, Selvin PR, Lu Y (2012) Angewandte Chemie International Edition 51: 6121

58. Jiang G, Pichaandi J, Johnson NJJ, Burke RD, van Veggel FCJM (2012) Langmuir 28: 3239
59. Deng M, Tu N, Bai F, Wang L (2012) Chem. Mat. 24: 2592
60. Bogdan N, Vetrone F, Ozin GA, Capobianco JA (2011) Nano Lett. 11: 835
61. Wang M, Liu J-L, Zhang Y-X, Hou W, Wu X-L, Xu S-K (2009) Materials Letters 63: 325
62. Chen Z, Chen H, Hu H, Yu M, Li F, Zhang Q, Zhou Z, Yi T, Huang C (2008) J. Am. Chem. Soc. 130: 3023
63. Cooper DR, Kudinov K, Tyagi P, Hill CK, Bradforth SE, Nadeau JL (2014) Physical Chemistry Chemical Physics 16: 12441
64. Chen YC, Huang SC, Wang YK, Liu YT, Wu TK, Chen TM (2013) Chem.-Asian J. 8: 2652
65. Sukhorukov GB, Donath E, Davis S, Lichtenfeld H, Caruso F, Popov VI, Möhwald H (1998) Polymers for Advanced Technologies 9: 759
66. Wang L, Yan R, Huo Z, Wang L, Zeng J, Bao J, Wang X, Peng Q, Li Y (2005) Angewandte Chemie International Edition 44: 6054
67. Escudero A, Carrillo-Carrion C, Zyuzin MV, Ashraf S, Hartmann R, Núñez N, Ocana M, Parak WJ (2016) Nanoscale
68. Guerrero-Martínez A, Pérez-Juste J, Liz-Marzán LM (2010) Adv. Mater. 22: 1182
69. Hu H, Xiong L, Zhou J, Li F, Cao T, Huang C (2009) Chem.-Eur. J. 15: 3577
70. Gai S, Yang P, Li C, Wang W, Dai Y, Niu N, Lin J (2010) Advanced Functional Materials 20: 1166
71. Mader HS, Link M, Achatz DE, Uhlmann K, Li X, Wolfbeis OS (2010) Chem.-Eur. J. 16: 5416
72. Gargas DJ, Chan EM, Ostrowski AD, Aloni S, Altoe MVP, Barnard ES, Sanii B, Urban JJ, Milliron DJ, Cohen BE, Schuck PJ (2014) Nat Nano 9: 300
73. Sun L, Ge X, Liu J, Qiu Y, Wei Z, Tian B, Shi L (2014) Nanoscale 6: 13242
74. Cheng L, Yang K, Zhang S, Shao M, Lee S, Liu Z (2010) Nano Research 3: 722
75. Chen G, Shen J, Ohulchanskyy TY, Patel NJ, Kutikov A, Li Z, Song J, Pandey RK, Ågren H, Prasad PN, Han G (2012) ACS Nano 6: 8280
76. Wong H-T, Tsang M-K, Chan C-F, Wong K-L, Fei B, Hao J (2013) Nanoscale 5: 3465
77. Wu X, Zhang Y, Takle K, Bilsel O, Li Z, Lee H, Zhang Z, Li D, Fan W, Duan C, Chan EM, Lois C, Xiang Y, Han G (2016) ACS Nano 10: 1060
78. Gorris HH, Ali R, Saleh SM, Wolfbeis OS (2011) Adv. Mater. 23: 1652
79. Kumar M, Zhang P (2010) Biosensors and Bioelectronics 25: 2431
80. Saleh SM, Ali R, Hirsch T, Wolfbeis OS (2011) Journal of Nanoparticle Research 13: 4603
81. Liu C, Wang Z, Jia H, Li Z (2011) Chem. Commun. 47: 4661
82. Xu S, Xu S, Zhu Y, Xu W, Zhou P, Zhou C, Dong B, Song H (2014) Nanoscale 6: 12573
83. Harvey P, Oakland C, Driscoll MD, Hay S, Natrajan LS (2014) Dalton Trans. 43: 5265
84. Duan N, Wu S, Zhu C, Ma X, Wang Z, Yu Y, Jiang Y (2012) Anal. Chim. Acta 723: 1
85. Wu K, Cui J, Kong X, Wang Y (2011) Journal of Applied Physics 110: 053510
86. Li D, Wang Y, Zhang X, Yang K, Liu L, Song Y (2012) Optics Communications 285: 1925

87. Vetrone F, Naccache R, Zamarrón A, Juarranz de la Fuente A, Sanz-Rodríguez F, Martinez Maestro L, Martín Rodriguez E, Jaque D, García Solé J, Capobianco JA (2010) ACS Nano 4: 3254
88. Sedlmeier A, Achatz DE, Fischer LH, Gorris HH, Wolfbeis OS (2012) Nanoscale 4: 7090
89. Liu X, Wang Y, Wang J, Zhang E, Xiong L, Zhao W (2009) Lasers & Electro Optics & The Pacific Rim Conference on Lasers and Electro-Optics, 2009. CLEO/PACIFIC RIM '09. Conference on p 1
90. Zhou P, Wang X, Ma Y, Lü H, Liu Z (2012) Laser Physics 22: 1744
91. Sayed FN, Grover V, Sudarsan V, Pandey BN, Asthana A, Vatsa RK, Tyagi AK (2012) J. Colloid Interface Sci. 367: 161
92. Nathan CG, Kristin AD, Ram S (2013) Annual Review of Materials Research 43: 481
93. Li Y, Zhang J, Luo Y, Zhang X, Hao Z, Wang X (2011) J. Mater. Chem. 21: 2895
94. (2012) Rare Earth Nanotechnology. Pan Stanford Publishing Pte.Ltd., Singapore
95. Das S, Yang C-Y, Lu C-H (2013) J. Am. Ceram. Soc. 96: 1602
96. Soares MRN, Soares MJ, Fernandes AJS, Rino L, Costa FM, Monteiro T (2011) J. Mater. Chem. 21: 15262
97. Klampaftis E, Ross D, McIntosh KR, Richards BS (2009) Solar Energy Materials and Solar Cells 93: 1182
98. Huang CK, Chen YC, Hung WB, Chen TM, Sun KW, Chang WL (2013) Progress in Photovoltaics: Research and Applications 21: 1507
99. Naccache R, Vetrone F, Capobianco JA (2013) ChemSusChem 6: 1308
100. Yuan C, Chen G, Prasad PN, Ohulchanskyy TY, Ning Z, Tian H, Sun L, Agren H (2012) J. Mater. Chem. 22: 16709
101. Yuan C, Chen G, Li L, Damasco JA, Ning Z, Xing H, Zhang T, Sun L, Zeng H, Cartwright AN, Prasad PN, Ågren H (2014) ACS Applied Materials & Interfaces 6: 18018